Research article

Differences in cortical microstructure according to body mass index in neurologically healthy populations using structural magnetic resonance imaging

Yunseo Park [a], Jong Young Namgung [a], Chae Yeon Kim [a], Yeongjun Park [b], Bo-yong Park [a,c,d,*]

[a] *Department of Data Science, Inha University, Incheon, Republic of Korea*
[b] *Department of Electrical and Computer Engineering, Sungkyunkwan University, Suwon, Republic of Korea*
[c] *Department of Statistics and Data Science, Inha University, Incheon, Republic of Korea*
[d] *Center for Neuroscience Imaging Research, Institute for Basic Science, Suwon, Republic of Korea*

ARTICLE INFO

ABSTRACT

Associations between brain structure and body mass index (BMI) are increasingly gaining attention. Although BMI-related regional alterations in brain morphology have been previously reported, the effect of BMI on the microstructural profiles, which provide information on the proxy of neuronal density within the cortex, is unexplored. In this study, we investigated the links between cortical layer-specific microstructural profiles and BMI in 302 neurologically healthy young adults. Using the microstructure-sensitive proxy based on the T1-and T2-weighted ratio, we estimated microstructural profile covariance (MPC) by calculating linear correlations of cortical depth-wise intensity profiles between different brain regions. Then, low-dimensional gradients of the MPC matrix were estimated using dimensionality reduction techniques, and the gradients were associated with BMI. Significant effects in the heteromodal association areas were observed. The BMI-gradient association map was related to the geodesic distance along the cortical surface, curvature, and sulcal depth, suggesting that the microstructural alterations occurred along the cortical topology. The BMI-gradient association map was further linked to cognitive states related to negative emotions. Our findings may provide insights into understanding the atypical cortical microstructure associated with BMI.

1. Introduction

Body mass index (BMI) is a metric that is used to assess the degree of obesity [1]. Individuals can be categorized as underweight (BMI≤18.5), healthy weight (18.5≤BMI<25), overweight (25≤BMI<30), or obese (BMI≥30) based on the BMI calculations. Individuals with a high BMI are susceptible to various health-related problems, such as type 2 diabetes, cardiovascular diseases, stroke, and cancer [1]. Brain studies have found that a high BMI is associated with altered brain mechanisms. For example, individuals with high BMI showed hormone imbalances and atypical functions in eating behavior-related brain circuits [2]. Previous neuroimaging studies have assessed BMI-related structural and functional brain alterations using magnetic resonance imaging (MRI) [3,4].

Moreover, as the BMI increases, the overall gray matter volume and cortical thickness reduce, and the curvature increases, affirming the association between cortical morphology and BMI [4–10]. Some studies have shown that individuals with a high BMI had decreased white matter integrity [3,4], indicating a relationship between microstructural alterations and BMI. These studies highlight the relationship between BMI and alterations in brain morphology and microstructure. However, comprehensive research delineating the relationship between BMI and cortical microstructure remains to be investigated. In this study, we aimed to examine the alterations in the cortical microstructure across varying BMI ranges.

Brain microstructure can be indirectly assessed *in vivo* using a microstructure-sensitive proxy based on the T1-and T2-weighted ratio [11,12]. A recent study provided a method to estimate cortical microstructure by sampling cortical gray matter into several equivolumetric layers and stratifying the intensity values of microstructure-sensitive proxy across the cortical layers [13]. The study provided a better understanding of the cortical microstructure by leveraging dimensionality reduction techniques. In that study, the microstructural profile covariance (MPC) was calculated by assessing inter-regional similarities in the microstructural profile, and a low-dimensional principal component (i.e., gradient) was generated using dimensionality reduction techniques [13]. This approach has an advantage in analyzing high-dimensional connectome data by generating principal components without losing substantial information of the original data. Additionally, the estimated low-dimensional gradients are robust to noise and biologically interpretable [13]. For example, this microstructural gradient demonstrated remarkable consistency across diverse datasets, further supporting its utility by showing the hierarchical organization along the cortex with a sensory-fugal axis [13]. This pattern was further related to gene expressions and functional dynamics in young adulthood and adolescent development [14]. Our previous work demonstrated associations between atypical brain hierarchy and obesity-related phenotypes [15,16]. Hence, we hypothesized that the microstructural gradient analysis might provide insights into understanding BMI-associated alterations in cortical microstructure.

In this study, we used T1- and T2-weighted MRI data of neurologically healthy young adults obtained from the Human Connectome Project (HCP) database to generate microstructural gradients and studied their associations with BMI. Further, we assessed relations between BMI and gradients to cortical morphology to identify the topology of the microstructure-BMI associations and performed meta-analytic cognitive decoding to infer related cognitive functions.

2. Methods

2.1. Participants

We studied neurologically healthy young adults obtained from the S1200 release of the HCP database (http://www.humanconnectome.org/) [17]. Among 1206 participants, we excluded participants who were genetically related (i.e., twins), had a family history of mental illness, a history of drug ingestion, and incomplete T1- and T2-weighted imaging data. Finally, 302 participants (mean $\pm$ standard deviation [SD] age $= 28.3 \pm 4.0$ years; 51.7 % female) were included in this study (Table 1). The mean $\pm$ SD of BMI was 26.01 ± 4.82 kg/m^2 and within a range of 17.01 and 42.91 kg/m^2. All data used in this study were publicly available and anonymized. Participant recruitment procedures and the informed consent forms (including consent to share deidentified data) were previously approved by the Washington University Institutional Review Board as part of the HCP, and the HCP team approved access to the data.

2.2. MRI data acquisition

The T1- and T2-weighted MRI were obtained using a Siemens Skyra 3T scanner at Washington University. The T1-weighted images were acquired using a magnetization-prepared rapid gradient echo (MPRAGE) sequence (repetition time [TR] $= 2400$ ms; echo time [TE] $= 2.14$ ms; field of view $= 224 \times 224$ mm^2; voxel size $= 0.7$ mm^2; number of slices $= 256$), and the T2-weighted data were scanned using a T2-SPACE sequence, where the parameters were the same as the T1-weighted data except for TR (3200 ms) and TE (565 ms).

2.3. MRI data preprocessing

The HCP database provided minimally preprocessed MRI data using FSL, FreeSurfer, and Workbench [18–20]. In brief, the T1- and T2-weighted images were corrected for gradient nonlinearity and b0 distortions and coregistered using a rigid-body transformation. Bias field correction was performed based on the inverse intensities from the T1- and T2-weighting. The processed data were non-linearly registered to the Montreal Neurological Institute (MNI152) standard space, and white and pial surfaces were generated by

Table 1
Demographic information of study participants.

	Underweight (BMI<18.5)	Healthy weight (18.5≤BMI<25)	Overweight (25≤BMI<30)	Obese (BMI≥30)
N	5	137	102	58
Age (mean $\pm$ SD, years)	28.4 ± 5.27	28.12 ± 4.12	28.16 ± 3.70	29.2 ± 4.03
Sex (male: female, %)	0 : 100	43 : 57	60 : 40	45 : 55
BMI (mean $\pm$ SD, kg/m^2)	17.76 ± 0.58	22.2 ± 1.62	27.18 ± 1.46	33.67 ± 3.14

Abbreviations: SD, standard deviation; BMI, body mass index.

following the boundaries between different tissues [21–23]. The mid-thickness surface was generated by averaging the pial and white surfaces, and it was used to create the inflated surface. The spherical surface was registered to the Conte69 template with 164k vertices using MSMAll [24,25] and downsampled to a 32k vertex mesh.

2.4. MPC matrix construction

First, we estimated the microstructure-sensitive proxy based on the ratio of the T1- and T2-weighted contrast [13]. We divided the cortex into 14 equivolumetric layers and sampled the microstructure-sensitive proxy along these surfaces [13]. The MPC matrix was constructed by calculating linear correlations of cortical depth-dependent T1w/T2w intensity profiles between different cortical regions defined using a Schaefer atlas with 300 parcels [26] while controlling for the average whole-cortical intensity profile [13]. The matrix was set at a threshold value of zero and log-transformed [13].

2.5. Microstructural gradient calculation

The group-level MPC matrix was generated by averaging the matrices across individuals. Then, we estimated microstructural gradients using nonlinear dimensionality reduction techniques [13]. Specifically, we constructed an affinity matrix with a normalized angle kernel with each parcel's top 10 % elements. The low-dimensional eigenvectors (i.e., gradients) of the affinity matrix were generated using the diffusion map embedding [27] implemented in the BrainSpace toolbox (https://github.com/MICA-MNI/BrainSpace) [28]. The generated individual participant-level microstructural gradients were aligned to the group-level gradient using Procrustes alignment [29].

2.6. Associations between BMI and microstructural gradients

Leveraging nonparametric permutation tests, we studied the associations between BMI and the first two gradients, which explained enough information on the MPC matrix after controlling for age and sex. The subject indices of microstructural gradients were randomly shuffled, and a linear model was constructed to fit the multivariate data (number of participants × number of brain regions × number of gradients) to BMI using a BrainStat toolbox (https://github.com/MICA-MNI/BrainStat) [30]. We repeated this process 10,000 times, and a null distribution was constructed. If the actual t-statistic (Hotelling's T^2) did not fall within 95 % of the null distribution, it was deemed significant. Multiple comparisons across brain regions were corrected using a false discovery rate (FDR) < 0.05 [31]. For a sensitivity analysis, we evaluated the between-group differences in the microstructural gradients of healthy weight (18.5≤BMI<25) and obese individuals (BMI≥30) based on the permutation tests. We randomly assigned the subject indices and implemented the multivariate linear models based on Hotelling's T statistics after controlling for age and sex from the microstructural gradients. This process was repeated 10,000 times, and a null distribution was established. Significance was determined if the actual t-statistic did not fall within 95 % of the null distribution. Multiple comparisons across brain regions were corrected using FDR <0.05 [31].

2.7. Topological analysis

To identify the topological underpinnings of the BMI-microstructural gradient associations, we calculated cortical thickness, curvature, sulcal depth, and geodesic distance. Cortical thickness is the distance between pial and white surfaces, which provides the thickness of the gray matter. Curvature is the degree of folding of the cortical surface and is used to quantify cortical gyrification. Sulcal depth is the vertical distance between the sulci and pial surfaces. Geodesic distance is the shortest path between different vertices along the cortical surface. We calculated linear correlations between the BMI-gradient association map and each cortical topology map. The significance was evaluated using 10,000 spin permutation tests [32], and multiple comparisons across topological maps were corrected using FDR <0.05 [31].

2.8. Meta-analytic cognitive decoding

We conducted a cognitive decoding analysis using NeuroSynth [33], implemented in the BrainStat toolbox [30]. NeuroSynth is a platform that provides cognitive terms related to input brain maps by performing a meta-analysis. Specifically, NeuroSynth provides statistical maps representing the likelihood of a specific term being related to brain activations, allowing us to evaluate the similarities between the input and activation maps derived from multiple neuroimaging studies. In this study, we decoded the BMI-gradient association map to identify related cognitive terms.

2.9. Statistical analysis

We performed a multivariate association analysis between BMI and microstructural gradients. After controlling for age and sex from the microstructural gradients, we repeated the multivariate analysis with 1000 permutation tests. Subject indices were randomly shuffled, and a null distribution of the association was established. P-value was calculated by dividing the number of permuted t-statistic values, which were larger than the real t-statistic values, by the number of permutations. Multiple comparisons across brain regions were corrected using FDR <0.05 [31]. A correlation analysis between the BMI-microstructural gradient association and

cortical morphologies, including cortical thickness, curvature, sulcal depth, and geodesic distance, was performed based on 10,000 spin permutation tests to account for spatial autocorrelation [32]. Multiple comparisons across cortical morphologies were corrected using FDR <0.05 [31].

3. Results

3.1. Microstructural gradients

Studying the T1- and T2-weighted MRI of 302 young neurologically healthy adults obtained from the HCP database [17], we leveraged dimensionality reduction techniques [27,28] to estimate microstructural gradients. The first two gradients explained approximately 70.2 % of the connectome information (Fig. 1A). The first gradient (explained 42.2 % of information) described the sensory-fugal axis expanding from the visual/motor regions to the default mode and frontoparietal areas. The second gradient (explained 28.0 % of the information) showed the anterior-posterior pattern.

3.2. Associations between BMI and microstructural gradients

We assessed associations between BMI and the estimated two microstructural gradients. Significant (FDR <0.05) effects were observed in the temporal pole and inferior parietal regions (Fig. 1B–C). When we stratified the effects according to four cortical hierarchical levels and seven functional communities, visual, limbic, and dorsal attention networks (i.e., idiotypic and heteromodal association areas) showed strong effects. When we assessed the between-group differences in the microstructural gradients between individuals with healthy weight (18.5≤BMI<25) and obesity (BMI≥30), largely consistent results were found (Pearson's r = 0.75, p_{spin} < 0.001; Supplementary Fig. 1).

3.3. Topological underpinnings

For the correlations between the BMI-gradient association map and multiple cortical morphological measures, significant relations with the geodesic distance (r = 0.17, $p_{spin-FDR}$ = 0.023), curvature (r = 0.14, $p_{spin-FDR}$ < 0.001), and sulcal depth (r = 0.19, $p_{spin-FDR}$ < 0.001) were observed. However, the correlation with cortical thickness was not statistically significant (r = 0.04, $p_{spin-FDR}$ = 0.803; Fig. 2). Our results suggest that the BMI-microstructure gradient associations are partially related to cortical morphology.

3.4. Cognitive decoding

We performed a meta-analytic cognitive decoding analysis to identify the potential cognitive functions associated with BMI-related
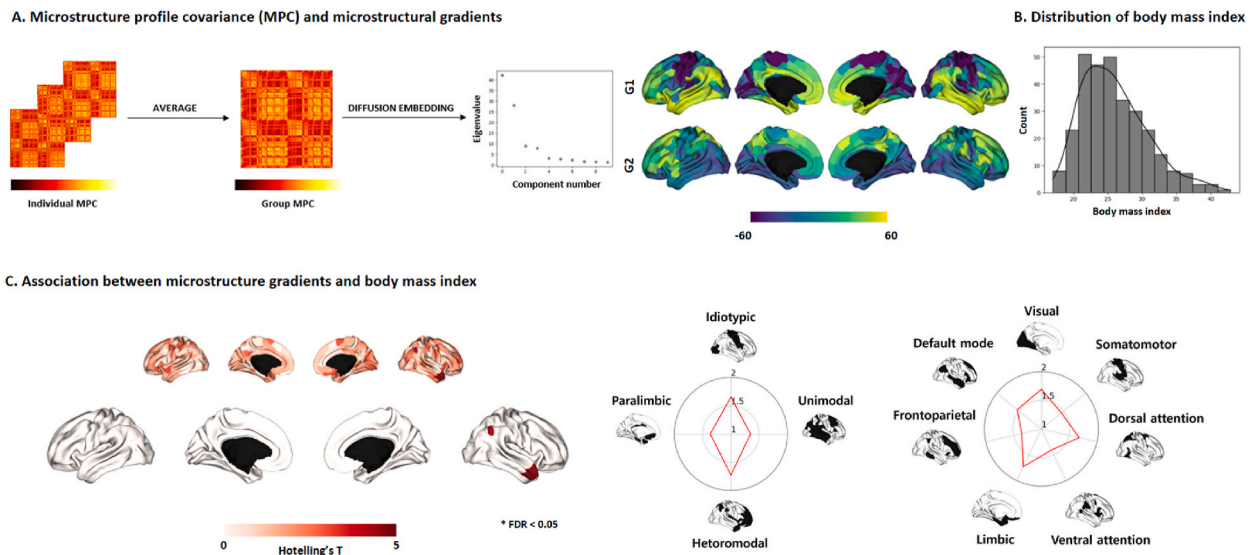
Fig. 1. Microstructural gradients and associations with body mass index. **(A)** Schema of generating microstructure gradients. Individual microstructural profile covariance (MPC) matrices were averaged, and dimensionality reduction techniques were applied to the group-level MPC matrix (left). The scree plot shows the eigenvalue of each component. We selected the first two gradients (G1 and G2), which explained approximately 70.2 % of the information. **(B)** The distribution of body mass index is reported with a histogram. **(C)** Associations between body mass index and microstructural gradients of the whole brain (left top) and regions that showed significant effects are shown (left bottom). The effects were stratified according to cortical hierarchy levels (middle) and intrinsic functional communities (right). Abbreviation: FDR, false discovery rate.

Fig. 2. Topological associations. A schema of topological measures is described (left). We calculated linear correlations between the body mass index-microstructure association maps and geodesic distance, cortical thickness, curvature, and sulcal depth.

cortical microstructural differences. Multiple terms were observed, such as conditioning, neutral, stimuli, stress, threat, nociceptive, dementia, pain, etc., and the negative terms (e.g., stress, nociceptive, and threat) were dominant (Fig. 3).

4. Discussion

A BMI-brain relationship is crucial to understand the neurobiological aspects of obesity. In this study, we investigated the differences in cortical microstructures across a wide range of BMI using microstructural gradient analysis. We found that higher-order heteromodal association cortices were altered according to BMI. A topological analysis revealed that BMI-related microstructural differences may follow cortical morphology of geodesic distance, curvature, and sulcal depth. Finally, these microstructural alterations were related to negative emotional states. Our findings suggested that cortical microstructural characteristics are linked to BMI and are associated with negative emotions.

The primary feature of our study was the microstructural gradients, which were the low-dimensional representations of the cortical microstructural profiles [13]. The first gradient delineated the sensory-fugal axis expanding from the visual and motor regions to the default mode and frontoparietal areas, indicating discernible variations in cortical lamination and myelin contents. The sensory regions exhibit pronounced laminar differentiation and high myelin content, whereas heteromodal association areas show less distinct lamination and low myelin content [13,34,35]. The second gradient showed the anterior-posterior axis, commonly observed in neuronal streamlines linking prefrontal and parietal/occipital regions [36]. In this study, we observed alterations in these microstructural gradients according to BMI. Particularly, the heteromodal association areas showed significant shifts in cortical microstructural profiles. The heteromodal association areas included default mode and frontoparietal cortices. These regions integrate information transferred from various sensory regions, and this sensory-heteromodal circuit is closely linked to individuals' higher-order cognitive functions [13]. Alterations in this system are highly associated with brain mechanisms related to eating behaviors, which might lead to disinhibited eating and obesity [34]. Our findings complement previously published studies by providing insights into BMI-related cortical microstructure and its potential links to cognitive functions.

The association analysis with cortical morphologies provided topological underpinnings of the BMI-microstructure associations. Cortical morphological features provide information on cortical topology and cognitive ability [35,37–39]. For example, geodesic distance reflected functional hierarchy differentiating sensory and transmodal (i.e., default mode and frontoparietal) regions [39,40]. The positive correlations between geodesic distance and BMI-microstructural gradient association map indicated alterations in brain

Fig. 3. Cognitive decoding analysis. We performed meta-analysis-based cognitive decoding, and the terms that showed strong correlations were plotted using large fonts.

microstructure, particularly in the transmodal regions compared to the sensory areas. The cortical curvature and sulcal depth also exhibited consistent results. Collectively, these findings suggest that cortical microstructure is more susceptible to BMI in higher-order default mode regions.

Moreover, cognitive decoding analysis revealed that microstructural alterations associated with BMI might be related to negative emotional states, such as pain, stress, and threat. Our previous work found that activation of the brain regions related to reward processing was associated with negative emotions [41], and other studies have shown that obesity is linked to an increased prevalence of negative emotional states, which can exacerbate eating behavior and contribute to a cycle of weight gain and emotional distress [42, 43]. These studies highlight the importance of BMI management for maintaining physical and mental health.

To our knowledge, this is the first study to investigate the associations between BMI and microstructural gradients representing the principal axis of cortical layer-wise microstructural profiles. This approach provided a compact way to link brain-behavior relationships by estimating low-dimensional representations of the microstructural organization of the brain. We also offered a multilevel framework consolidating microstructural profiles, topological characteristics, and cognitive functions to unveil BMI-related brain alterations. This framework may offer insights into identifying neuroimaging markers related to obesity.

Our study has some limitations. Due to the unavailability of data in the database, we did not control for potential confounding factors, such as physical activity and dietary habits, which might influence the associations between BMI and cortical microstructure. Thus, caution needs to be applied when interpreting the results of this study because the influence of these unmeasured variables cannot be ruled out. Future studies could investigate the role of these potential confounders more comprehensively on the associations between BMI and cortical microstructure. Additionally, our findings do not provide information on whether negative emotions affected the increase in BMI because our analysis assessed the relationship and not causality. Future works are required to evaluate the causal links between emotional states and BMI.

Our study investigated cortical microstructure alterations according to BMI using dimensionality reduction techniques. We pointed out that higher-order heteromodal association areas are susceptible to BMI, and the alterations are related to negative cognitive states. Our study provides insights into understanding the relationship between BMI and cortical microstructure and also highlights the importance of managing BMI.

Data availability statement

Imaging and phenotypic data were provided, in part, by the Human Connectome Project (HCP; http://www.humanconnectome.org/).

Code availability statement

The codes for gradient generation are available at https://github.com/MICA-MNI/BrainSpace, and statistical analyses are at https://github.com/MICA-MNI/BrainStat.

Funding

CRediT authorship contribution statement

Yunseo Park: Writing – original draft, Visualization, Validation, Methodology, Investigation, Formal analysis, Data curation, Conceptualization. **Jong Young Namgung:** Writing – review & editing, Methodology, Investigation. **Chae Yeon Kim:** Writing – review & editing, Validation, Methodology. **Yeongjun Park:** Writing – review & editing, Methodology. **Bo-yong Park:** Writing – review & editing, Writing – original draft, Visualization, Validation, Supervision, Software, Resources, Project administration, Methodology, Investigation, Funding acquisition, Formal analysis, Data curation, Conceptualization.

Declaration of competing interest

The authors declare that they have no known competing financial interests or personal relationships that could have appeared to influence the work reported in this paper.

Appendix A. Supplementary data

Supplementary data to this article can be found online at https://doi.org/10.1016/j.heliyon.2024.e33134.

References

[1] World Health Organization, Obesity and Overweight, 2021.
[2] E.B. Lee, M.P. Mattson, The neuropathology of obesity: insights from human disease, Acta Neuropathol. 127 (2014) 3–28, https://doi.org/10.1007/s00401-013-1190-x.
[3] J. Xu, Y. Li, H. Lin, R. Sinha, M.N. Potenza, Body mass index correlates negatively with white matter integrity in the fornix and corpus callosum: a diffusion tensor imaging study, Hum. Brain Mapp. 34 (2013) 1044–1052, https://doi.org/10.1002/hbm.21491.
[4] K.A. Carbine, K.M. Duraccio, A. Hedges-Muncy, K.A. Barnett, C.B. Kirwan, C.D. Jensen, White matter integrity disparities between normal-weight and overweight/obese adolescents: an automated fiber quantification tractography study, Brain Imaging Behav 14 (2020) 308–319, https://doi.org/10.1007/s11682-019-00036-4.
[5] Y. Taki, S. Kinomura, K. Sato, K. Inoue, R. Goto, K. Okada, S. Uchida, R. Kawashima, H. Fukuda, Relationship between body mass index and Gray Matter Volume in 1,428 healthy individuals, Obesity 16 (2008) 119–124, https://doi.org/10.1038/oby.2007.4.
[6] N. Medic, H. Ziauddeen, K.D. Ersche, I.S. Farooqi, E.T. Bullmore, P.J. Nathan, L. Ronan, P.C. Fletcher, Increased body mass index is associated with specific regional alterations in brain structure, Int. J. Obes. 40 (2016) 1177–1182, https://doi.org/10.1038/ijo.2016.42.
[7] N. Medic, P. Kochunov, H. Ziauddeen, K.D. Ersche, P.J. Nathan, L. Ronan, P.C. Fletcher, BMI-related cortical morphometry changes are associated with altered white matter structure, Int. J. Obes. 43 (2019) 523–532, https://doi.org/10.1038/s41366-018-0269-9.
[8] M.J. Herrmann, A.K. Tesar, J. Beier, M. Berg, B. Warrings, Grey matter alterations in obesity: a meta-analysis of whole-brain studies, Obes. Rev. 20 (2019) 464–471, https://doi.org/10.1111/obr.12799.
[9] I. Marqués-Iturria, R. Pueyo, M. Garolera, B. Segura, C. Junqué, I. García-García, M. José Sender-Palacios, M. Vernet-Vernet, A. Narberhaus, M. Ariza, M.Á. Jurado, Frontal cortical thinning and subcortical volume reductions in early adulthood obesity, Psychiatry Res. Neuroimaging. 214 (2013) 109–115, https://doi.org/10.1016/j.pscychresns.2013.06.004.
[10] M.E. Shott, M.A. Cornier, V.A. Mittal, T.L. Pryor, J.M. Orr, M.S. Brown, G.K.W. Frank, Orbitofrontal cortex volume and brain reward response in obesity, Int. J. Obes. 39 (2015) 214–221, https://doi.org/10.1038/ijo.2014.121.
[11] M.F. Glasser, M.S. Goyal, T.M. Preuss, M.E. Raichle, D.C. Van Essen, Trends and properties of human cerebral cortex: correlations with cortical myelin content, Neuroimage 93 (2014) 165–175, https://doi.org/10.1016/j.neuroimage.2013.03.060.
[12] M.F. Glasser, D.C. van Essen, Mapping human cortical areas in vivo based on myelin content as revealed by T1- and T2-weighted MRI, J. Neurosci. 31 (2011) 11597–11616, https://doi.org/10.1523/JNEUROSCI.2180-11.2011.
[13] C. Paquola, R. Vos De Wael, K. Wagstyl, R.A.I. Bethlehem, S.J. Hong, J. Seidlitz, E.T. Bullmore, A.C. Evans, B. Misic, D.S. Margulies, J. Smallwood, B.C. Bernhardt, Microstructural and functional gradients are increasingly dissociated in transmodal cortices, PLoS Biol. 17 (2019), https://doi.org/10.1371/journal.pbio.3000284.
[14] C. Paquola, R.A. Bethlehem, J. Seidlitz, K. Wagstyl, R. Romero-Garcia, K.J. Whitaker, R. Vos De Wael, G.B. Williams, N. Consortium, P.E. Vé Rtes, D.S. Margulies, B. Bernhardt, E.T. Bullmore, Shifts in myeloarchitecture characterise adolescent development of cortical gradients, Elife 8 (2019) e50482, https://doi.org/10.7554/eLife.50482.001.
[15] B. yong Park, H. Park, F. Morys, M. Kim, K. Byeon, H. Lee, S.H. Kim, S.L. Valk, A. Dagher, B.C. Bernhardt, Inter-individual body mass variations relate to fractionated functional brain hierarchies, Commun. Biol. 4 (2021), https://doi.org/10.1038/s42003-021-02268-x.
[16] H. Lee, J. Kwon, J. eun Lee, B. yong Park, H. Park, Disrupted stepwise functional brain organization in overweight individuals, Commun. Biol. 5 (2022), https://doi.org/10.1038/s42003-021-02957-7.
[17] D.C. Van Essen, S.M. Smith, D.M. Barch, T.E.J. Behrens, E. Yacoub, K. Ugurbil, The Wu-Minn human connectome Project: an overview, Neuroimage 80 (2013) 62–79, https://doi.org/10.1016/j.neuroimage.2013.05.041.
[18] M. Jenkinson, C.F. Beckmann, T.E.J. Behrens, M.W. Woolrich, S.M. Smith, Fsl, Neuroimage 62 (2012) 782–790, https://doi.org/10.1016/j.neuroimage.2011.09.015.
[19] B. Fischl, FreeSurfer, Neuroimage 62 (2012) 774–781, https://doi.org/10.1016/j.neuroimage.2012.01.021.
[20] M.F. Glasser, S.N. Sotiropoulos, J.A. Wilson, T.S. Coalson, B. Fischl, J.L. Andersson, J. Xu, S. Jbabdi, M. Webster, J.R. Polimeni, D.C. Van Essen, M. Jenkinson, The minimal preprocessing pipelines for the Human Connectome Project, Neuroimage 80 (2013) 105–124, https://doi.org/10.1016/j.neuroimage.2013.04.127.
[21] A.M. Dale, B. Fischl, M.I. Sereno, Cortical surface-based analysis I. Segmentation and surface reconstruction. http://www.idealibrary.com, 1999.
[22] B. Fischl, M.I. Sereno, A.M. Dale, Cortical surface-based analysis II: inflation, flattening, and a surface-based coordinate system. http://www.idealibrary.com, 1999.
[23] B. Fischl, M.I. Sereno, R.B.H. Tootell, A.M. Dale, High-resolution intersubject averaging and a coordinate system for the cortical surface, Hum. Brain Mapp. 8 (1999) 272–284, https://doi.org/10.1002/(SICI)1097-0193(1999)8:4<272::AID-HBM10>3.0.CO, 2-4.
[24] D.C. Van Essen, M.F. Glasser, D.L. Dierker, J. Harwell, T. Coalson, Parcellations and hemispheric asymmetries of human cerebral cortex analyzed on surface-based atlases, Cerebr. Cortex 22 (2012) 2241–2262, https://doi.org/10.1093/cercor/bhr291.
[25] M.F. Glasser, T.S. Coalson, E.C. Robinson, C.D. Hacker, J. Harwell, E. Yacoub, K. Ugurbil, J. Andersson, C.F. Beckmann, M. Jenkinson, S.M. Smith, D.C. Van Essen, A multi-modal parcellation of human cerebral cortex, Nature 536 (2016) 171–178, https://doi.org/10.1038/nature18933.
[26] A. Schaefer, R. Kong, E.M. Gordon, T.O. Laumann, X.-N. Zuo, A.J. Holmes, S.B. Eickhoff, B.T.T. Yeo, Local-global parcellation of the human cerebral cortex from intrinsic functional connectivity MRI, Cerebr. Cortex 28 (2018) 3095–3114, https://doi.org/10.1093/cercor/bhx179.
[27] R.R. Coifman, S. Lafon, Diffusion maps, Appl. Comput. Harmon. Anal. 21 (2006) 5–30, https://doi.org/10.1016/j.acha.2006.04.006.
[28] R. Vos de Wael, O. Benkarim, C. Paquola, S. Lariviere, J. Royer, S. Tavakol, T. Xu, S.J. Hong, G. Langs, S. Valk, B. Misic, M. Milham, D. Margulies, J. Smallwood, B.C. Bernhardt, BrainSpace: a toolbox for the analysis of macroscale gradients in neuroimaging and connectomics datasets, Commun. Biol. 3 (2020), https://doi.org/10.1038/s42003-020-0794-7.
[29] G. Langs, P. Golland, S.S. Ghosh, Predicting activation across individuals with resting-state functional connectivity based multi-atlas label fusion, in: Lecture Notes in Computer Science (Including Subseries Lecture Notes in Artificial Intelligence and Lecture Notes in Bioinformatics), Springer Verlag, 2015, pp. 313–320, https://doi.org/10.1007/978-3-319-24571-3_38.
[30] S. Larivière, Ş. Bayrak, R. Vos de Wael, O. Benkarim, P. Herholz, R. Rodriguez-Cruces, C. Paquola, S.J. Hong, B. Misic, A.C. Evans, S.L. Valk, B.C. Bernhardt, BrainStat: a toolbox for brain-wide statistics and multimodal feature associations, Neuroimage 266 (2023), https://doi.org/10.1016/j.neuroimage.2022.119807.
[31] Y. Benjamini, Y. Hochberg, Controlling the false discovery rate: a practical and powerful approach to multiple testing, J. R. Stat. Soc. 57 (1995) 289–300.
[32] A.F. Alexander-Bloch, H. Shou, S. Liu, T.D. Satterthwaite, D.C. Glahn, R.T. Shinohara, S.N. Vandekar, A. Raznahan, On testing for spatial correspondence between maps of human brain structure and function, Neuroimage 178 (2018) 540–551, https://doi.org/10.1016/j.neuroimage.2018.05.070.
[33] T. Yarkoni, R.A. Poldrack, T.E. Nichols, D.C. Van Essen, T.D. Wager, Large-scale automated synthesis of human functional neuroimaging data, Nat. Methods 8 (2011) 665–670, https://doi.org/10.1038/nmeth.1635.
[34] D. Val-Laillet, E. Aarts, B. Weber, M. Ferrari, V. Quaresima, L.E. Stoeckel, M. Alonso-Alonso, M. Audette, C.H. Malbert, E. Stice, Neuroimaging and neuromodulation approaches to study eating behavior and prevent and treat eating disorders and obesity, Neuroimage Clin 8 (2015) 1–31, https://doi.org/10.1016/j.nicl.2015.03.016.
[35] N. Gogtay, J.N. Giedd, L. Lusk, K.M. Hayashi, D. Greenstein, A.C. Vaituzis, T.F. Nugent Iii, D.H. Herman, L.S. Clasen, A.W. Toga, J.L. Rapoport, P.M. Thompson, Dynamic mapping of human cortical development during childhood through early adulthood, Proc. Natl. Acad. Sci. USA 101 (2004) 8174–8179.
[36] A.M. Radwan, S. Sunaert, K. Schilling, M. Descoteaux, B.A. Landman, M. Vandenbulcke, T. Theys, P. Dupont, L. Emsell, An atlas of white matter anatomy, its variability, and reproducibility based on constrained spherical deconvolution of diffusion MRI, Neuroimage 254 (2022), https://doi.org/10.1016/j.neuroimage.2022.119029.

[37] P. Shaw, D. Greenstein, J. Lerch, L. Clasen, R. Lenroot, N. Gogtay, A. Evans, J. Rapoport, J. Giedd, Intellectual ability and cortical development in children and adolescents, Nature 440 (2006) 676–679, https://doi.org/10.1038/nature04513.

[38] D. van der Meer, T. Kaufmann, Mapping the genetic architecture of cortical morphology through neuroimaging: progress and perspectives, Transl. Psychiatry 12 (2022), https://doi.org/10.1038/s41398-022-02193-5.

[39] S. Oligschläger, J.M. Huntenburg, J. Golchert, M.E. Lauckner, T. Bonnen, D.S. Margulies, Gradients of connectivity distance are anchored in primary cortex, Brain Struct. Funct. 222 (2017) 2173–2182, https://doi.org/10.1007/s00429-016-1333-7.

[40] D.S. Margulies, S.S. Ghosh, A. Goulas, M. Falkiewicz, J.M. Huntenburg, G. Langs, G. Bezgin, S.B. Eickhoff, F.X. Castellanos, M. Petrides, E. Jefferies, J. Smallwood, Situating the default-mode network along a principal gradient of macroscale cortical organization, Proc Natl Acad Sci U S A 113 (2016) 12574–12579, https://doi.org/10.1073/pnas.1608282113.

[41] B.Y. Park, J. Hong, H. Park, Neuroimaging biomarkers to associate obesity and negative emotions, Sci. Rep. 7 (2017), https://doi.org/10.1038/s41598-017-08272-8.

[42] H. Yang, X. Zhou, L. Xie, J. Sun, The effect of emotion regulation on emotional eating among undergraduate students in China: the chain mediating role of impulsivity and depressive symptoms, PLoS One 18 (2023), https://doi.org/10.1371/journal.pone.0280701.

[43] A. Dakanalis, M. Mentzelou, S.K. Papadopoulou, D. Papandreou, M. Spanoudaki, G.K. Vasios, E. Pavlidou, M. Mantzorou, C. Giaginis, The association of emotional eating with overweight/obesity, depression, anxiety/stress, and dietary patterns: a review of the current clinical evidence, Nutrients 15 (2023), https://doi.org/10.3390/nu15051173.